Supplementary Information for "Quantifying key mechanisms that contribute to the deviation of the tropical warming profile from a moist adiabat"

Osamu Miyawaki[1], Zhihong Tan[2], Tiffany Shaw[1], Malte Jansen[1]

[1]Department of the Geophysical Sciences, The University of Chicago

[2]Program in Atmospheric and Oceanic Sciences, Princeton University

Contents of this file

1. Tables S1 to S5

2. Figures S1 to S8

Table S1. Overprediction in % of the moist adiabat across the CMIP5 hierarchy for individual models used in this study. Blank data denote models for which data was not available in the corresponding model configuration.

	AOGCM		AGCMp			AGCMu			AQUA		
	T	T-L	T	T-L	T-L-D	T	T-L	T-L-D	T	T-L	T-L-D
ACCESS1-0	10.6	7.6	–	–	–	–	–	–	–	–	–
ACCESS1-3	27.5	23.2	–	–	–	–	–	–	–	–	–
bcc-csm1-1	23.1	11.6	19.4	5.9	1.4	22.8	12.3	7.4	–	–	–
bcc-csm1-1-m	32.3	29.3	–	–	–	–	–	–	–	–	–
BNU-ESM	27.1	27.9	–	–	–	–	–	–	–	–	–
CanESM2	25.5	10.4	15.8	6.2	5.9	15.6	9.3	9.1	–	–	–
CCSM4	26.4	29.4	22.8	22.2	22.1	23.8	26.7	26.6	23.6	22.8	21.7
CNRM-CM5	46.9	46.2	40.3	39.5	32.1	40.2	39.8	31.4	52.0	51.5	43.0
CNRM-CM5-2	46.4	45.5	–	–	–	–	–	–	–	–	–
CSIRO-Mk3-6-0	28.0	9.6	–	–	–	–	–	–	–	–	–
FGOALS-g2	24.5	22.4	–	–	–	–	–	–	20.5	18.4	16.9
FGOALS-s2	35.5	24.6	–	–	–	–	–	–	–	–	–
GFDL-CM3	22.2	18.4	–	–	–	–	–	–	–	–	–
GFDL-ESM2G	31.4	30.5	–	–	–	–	–	–	–	–	–
GFDL-ESM2M	33.8	31.6	–	–	–	–	–	–	–	–	–
GISS-E2-H	23.8	19.8	–	–	–	–	–	–	–	–	–
GISS-E2-R	21.2	18.2	–	–	–	–	–	–	–	–	–
HadGEM2-ES	12.6	8.1	10.0	8.2	4.5	11.2	10.7	6.5	7.1	6.2	4.7
inmcm4	36.6	24.2	–	–	–	–	–	–	–	–	–
IPSL-CM5A-LR	27.1	21.0	21.0	11.0	8.6	21.1	21.5	19.5	22.4	21.8	21.8
IPSL-CM5A-MR	27.1	19.2	–	–	–	–	–	–	–	–	–
IPSL-CM5B-LR	13.4	6.1	12.3	11.0	−2.0	13.1	3.6	3.4	–	–	–
MIROC-ESM	8.2	−11.3	–	–	–	–	–	–	–	–	–
MIROC5	22.8	10.5	17.8	10.4	8.3	18.0	14.2	11.9	19.4	9.7	11.4
MPI-ESM-LR	16.5	11.1	16.0	9.6	1.8	18.5	13.1	4.4	−11.4	−4.3	−9.9
MPI-ESM-MR	16.9	10.0	19.6	13.0	4.4	21.3	16.2	6.6	−9.3	−4.6	−10.4
MPI-ESM-P	17.0	12.2	–	–	–	–	–	–	–	–	–
MRI-CGCM3	29.8	17.9	26.4	18.2	15.7	26.5	23.4	20.6	24.8	21.1	18.6
NorESM1-M	20.9	23.2	–	–	–	–	–	–	–	–	–
All model mean	25.3	19.2	20.1	13.0	9.3	21.1	17.3	13.4	16.6	15.9	13.1
AGCM-subset mean	23.7	16.6	20.1	13.0	9.3	21.1	17.3	13.4	16.1	15.5	12.6
AQUA-subset mean	24.8	19.5	21.7	16.5	12.2	22.6	20.7	15.9	16.6	15.9	13.1

Table S2. Overprediction in % of the moist adiabat across the model hierarchy for various types of the moist adiabat. Three types of moist adiabatic lapse rates are shown here following the definitions in the AMS glossary. *Standard*: The limit of a moist pseudoadiabat when $r_v \ll 1$ (AMS, cited 2020: Moist-adiabatic lapse rate). *Pseudoadiabat*: Moist pseudoadiabat, which assumes that all condensates precipitate immediately (AMS, cited 2020: pseudoadiabatic lapse rate). *Reversible*: Reversible moist-adiabat, which assumes that all condensates remain in the parcel (AMS, cited 2020: reversible moist-adiabatic process). Furthermore, we test the sensitivity of overprediction to the boundary condition of the moist adiabat by using the temperature, relative humidity, and pressure at 2 m and at 950 hPa. Finally, we show overprediction for the default adiabat where latent heat of sublimation from freezing is ignored (NF), and a modified adiabat where freezing is included (F) following the European Centre for Medium-Range Weather Forecasts Integrated Forecast System Documentation Cycle 40 as in Flannaghan et al. (2014).

	AOGCM		AGCMp			AGCMu			AQUA		
	T	T-L	T	T-L	T-L-D	T	T-L	T-L-D	T	T-L	T-L-D
Standard											
2 m											
NF	25.3	19.2	20.1	13.0	9.3	21.1	17.3	13.4	16.6	15.9	13.1
F	25.5	18.2	18.6	9.9	6.2	20.1	14.6	10.6	16.0	14.8	12.0
950 hPa											
NF	20.6	14.7	17.4	11.4	8.1	17.5	16.8	13.2	15.9	16.2	12.9
F	22.5	15.9	18.2	11.1	7.7	18.7	16.8	13.1	17.6	17.6	14.1
Pseudoadiabat											
2 m											
NF	30.5	24.6	25.2	18.1	14.4	26.3	22.6	18.6	22.4	21.7	18.8
F	30.1	22.9	23.1	14.3	10.5	24.7	19.3	15.1	21.2	20.0	17.0
950 hPa											
NF	25.3	19.6	22.0	16.2	12.8	22.2	21.7	18.1	21.1	21.6	18.1
F	26.9	20.4	22.5	15.4	11.9	23.1	21.3	17.6	22.6	22.6	19.0
Reversible											
2 m											
NF	24.7	18.3	19.0	11.5	7.7	20.1	15.9	11.9	15.7	14.8	11.9
F	28.4	20.9	21.0	11.9	8.0	22.7	16.8	12.7	19.2	17.8	14.8
950 hPa											
NF	21.1	14.7	17.3	10.7	7.3	17.5	16.2	12.6	16.3	16.4	12.9
F	26.2	19.3	21.4	13.7	10.3	22.1	19.8	16.1	21.6	21.4	17.8

Table S3. Same as Table S3 but for GFDLrce and GFDLaqua configured with varying Tokioka parameters (α). The default Tokioka parameter used in the GFDL models is $\alpha = 0.025$. In general, overprediction decreases with decreasing α.

	GFDLrce						GFDLaqua					
α	0	0.00625	0.0125	0.025	0.05	0.1	0	0.00625	0.0125	0.025	0.05	0.1
Standard												
2 m												
NF	6.7	7.0	8.9	11.6	13.3	17.1	8.3	8.8	10.0	13.2	14.8	17.9
F	8.3	8.1	9.9	12.3	13.9	17.3	8.3	8.7	9.9	13.0	14.2	16.4
950 hPa												
NF	5.8	7.0	8.2	10.2	13.6	15.6	8.2	6.1	9.9	11.6	15.7	22.6
F	7.9	8.9	10.0	11.7	14.6	16.2	8.7	6.7	10.5	12.0	15.9	22.5
Pseudoadiabat												
2 m												
NF	11.9	12.3	14.2	16.8	18.7	22.7	13.8	14.3	15.5	18.7	20.5	23.7
F	13.1	13.1	15.0	17.3	18.9	22.3	13.2	13.7	14.9	17.9	19.1	21.9
950 hPa												
NF	10.9	12.1	13.3	15.3	18.8	21.0	13.5	11.5	15.3	16.9	21.2	28.3
F	12.7	13.8	14.9	16.4	19.5	21.3	13.7	11.7	15.5	17.0	21.0	27.7
Reversible												
2 m												
NF	6.8	6.9	8.7	11.1	12.7	16.4	7.5	8.1	9.3	12.4	13.9	16.9
F	12.0	11.8	13.6	15.8	17.2	20.3	11.3	11.8	13.0	15.8	16.9	19.7
950 hPa												
NF	6.4	7.4	8.5	10.3	13.6	15.4	8.0	6.1	9.8	11.4	15.4	22.1
F	11.9	12.8	13.9	15.2	18.6	19.9	12.3	10.3	14.1	15.5	19.3	25.9

Table S4. P-values of the T-test for the null hypothesis that the difference in mean overprediction averaged over 10°N/S and averaged only over regions of strong mean ascent ($\omega < -35$ hPa/d) are indistinguishable from zero. The mean difference and the 5–95% confidence interval are also shown. The difference is statistically significant for model configurations that have zonally-asymmetric circulations. (p-value $< 5\%$, indicated in bold).

T - (T-L)	Lower Bound	Mean	Upper Bound	p-value
AOGCM	3.89	6.10	8.28	**0.0000**
AGCMp	4.03	7.15	10.28	**0.0005**
AGCMu	0.96	3.75	6.55	**0.0134**
AQUA	−2.94	0.72	4.38	0.6627

Table S5. P-values of the T-test for the null hypothesis that the difference in mean overprediction between the combined indirect plus the direct CO_2 response and only the indirect CO_2 response are indistinguishable from zero. The mean difference and the 5–95% confidence interval are also shown. The difference is statistically significant for all model configurations (p-value $< 5\%$, indicated in bold).

(T-L) - (T-L-D)	Lower Bound	Mean	Upper Bound	p-value
AGCMp	1.53	3.63	5.72	**0.0032**
AGCMu	1.54	3.94	6.33	**0.0043**
AQUA	0.31	2.80	5.28	**0.0317**

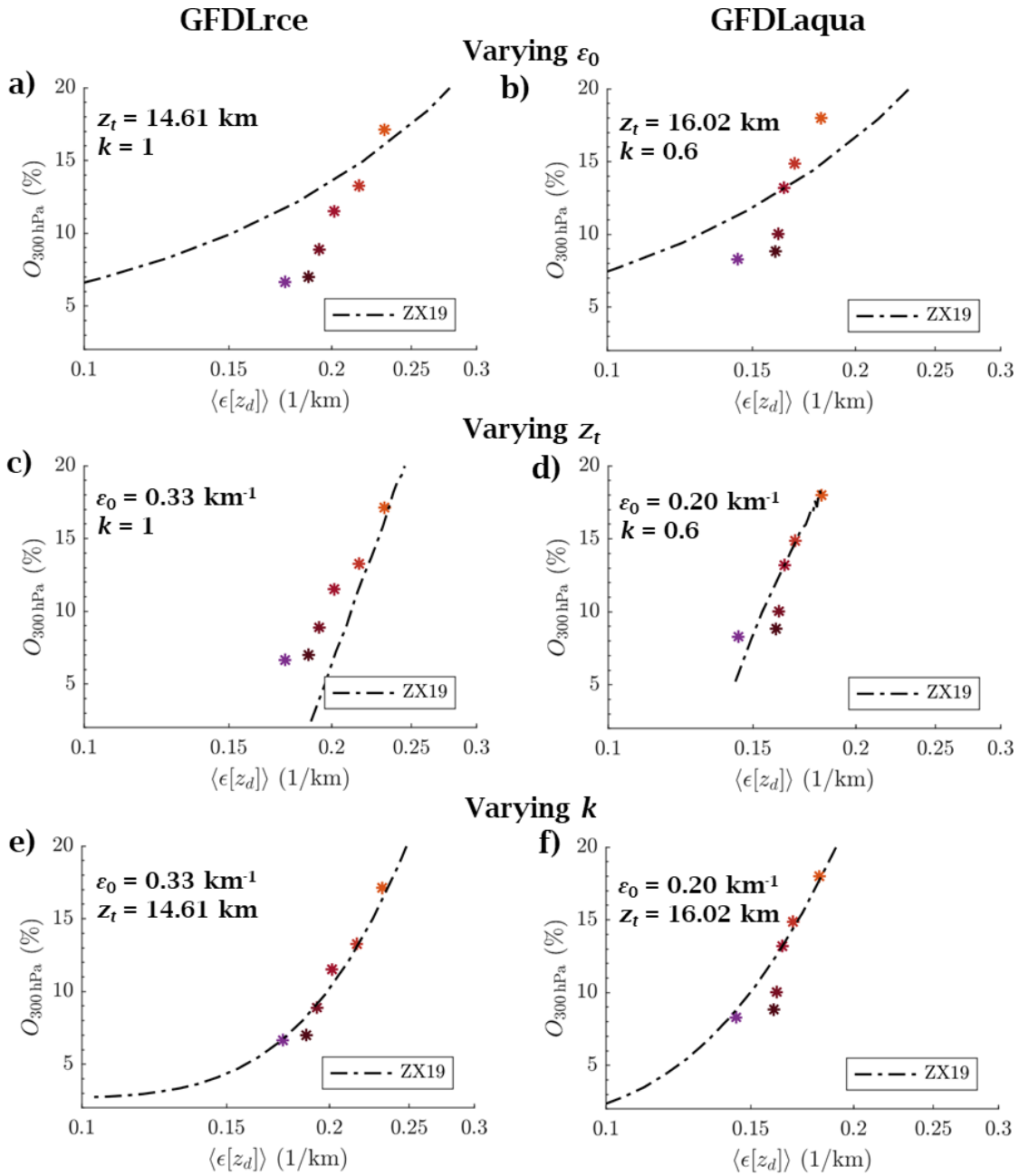

Figure S1. The relationship between spectral entrainment rate $\epsilon[z_d]$ and overprediction obtained by the ZX19 model are shown as dash-dot lines compared to the a) GFDLrce and b) GFDLaqua results where $\epsilon[z_d]$ in ZX19 is varied by varying ϵ_0 while holding z_t and k fixed. c) and d) are the same except $\epsilon[z_d]$ is varied by varying z_t while holding ϵ_0 and k fixed. For e) and f), $\epsilon[z_d]$ is varied by varying k while holding z_t and ϵ_0 fixed.

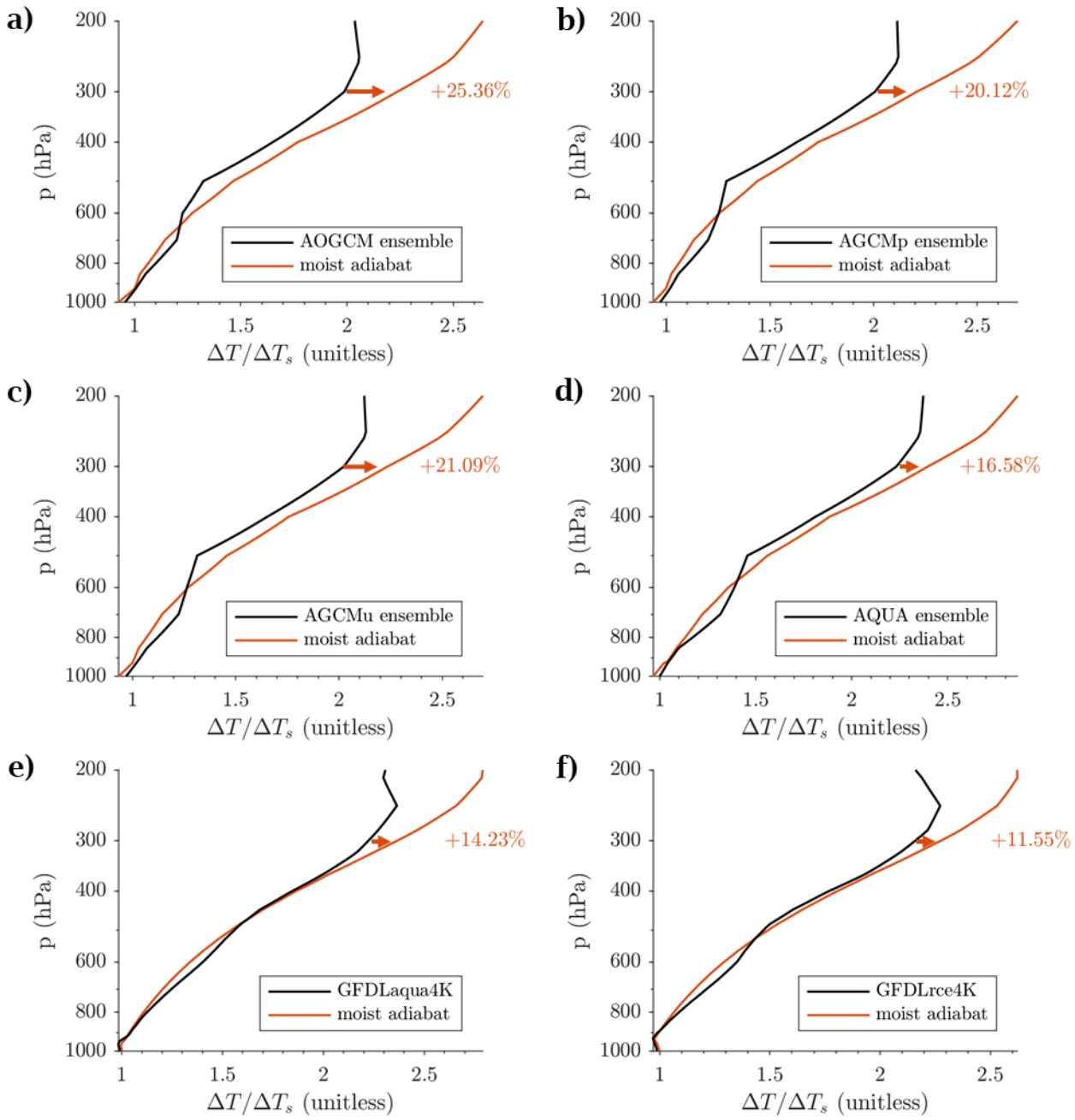

Figure S2. a) Vertical structure of the temperature response over the tropics (defined as 10°N/S) for the AOGCM multi-model mean (black) and the prediction based on a moist adiabat (orange). The moist adiabat overpredicts the AOGCM response by 25.34% at 300 hPa. b)–d) are the same for the AGCMp, AGCMu, and AQUA multi-model mean responses, respectively. e) and f) are the same for GFDLaqua4K and GFDLrce4K responses.

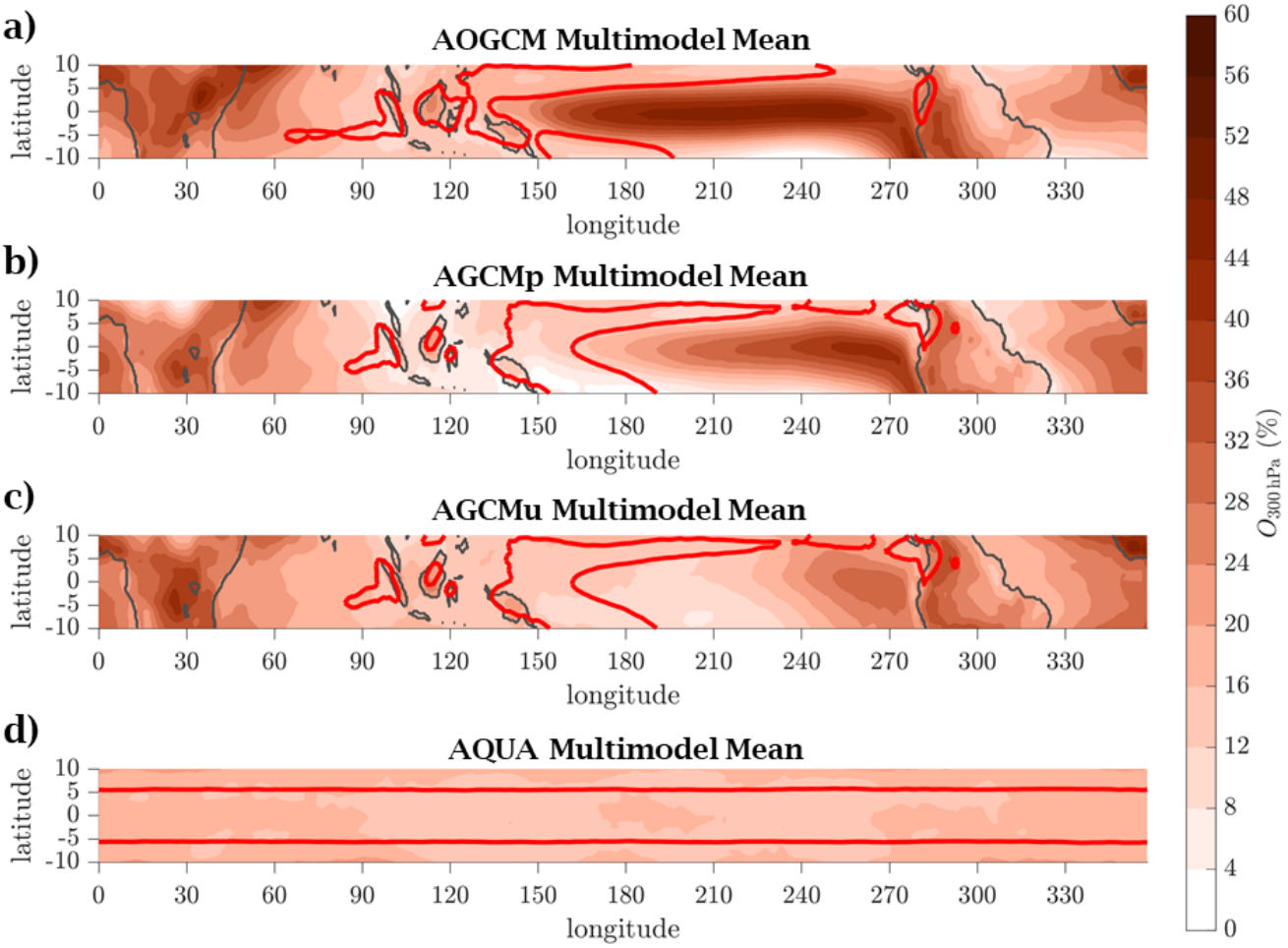

Figure S3. a) Spatial structure of the overprediction of the moist adiabat at 300 hPa in response to warming for the AOGCM multi-model mean. The red contour denotes the boundary of the multi-model mean climatological deep convection using precipitation of 8 mm/d as the criterion. b)–d) are the same for AGCMp, AGCMu, and AQUA, respectively.

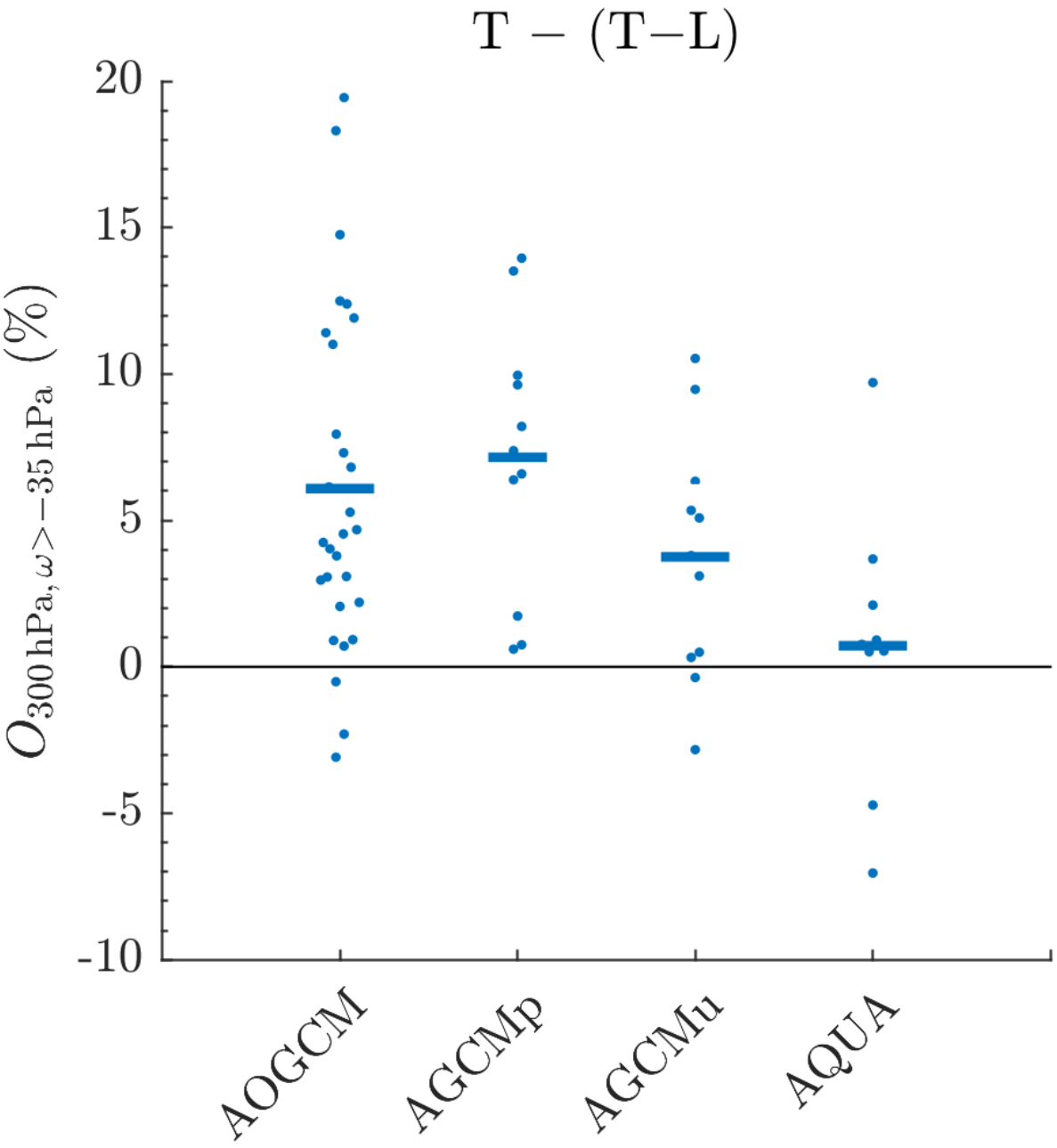

Figure S4. The difference between overprediction averaged over 10°N/S and overprediction averaged only over regions of climatological deep convection ($\omega < -35$ hPa/d) for each model across the model hierarchy (dots). The mean difference in overprediction is denoted by the horizontal line.

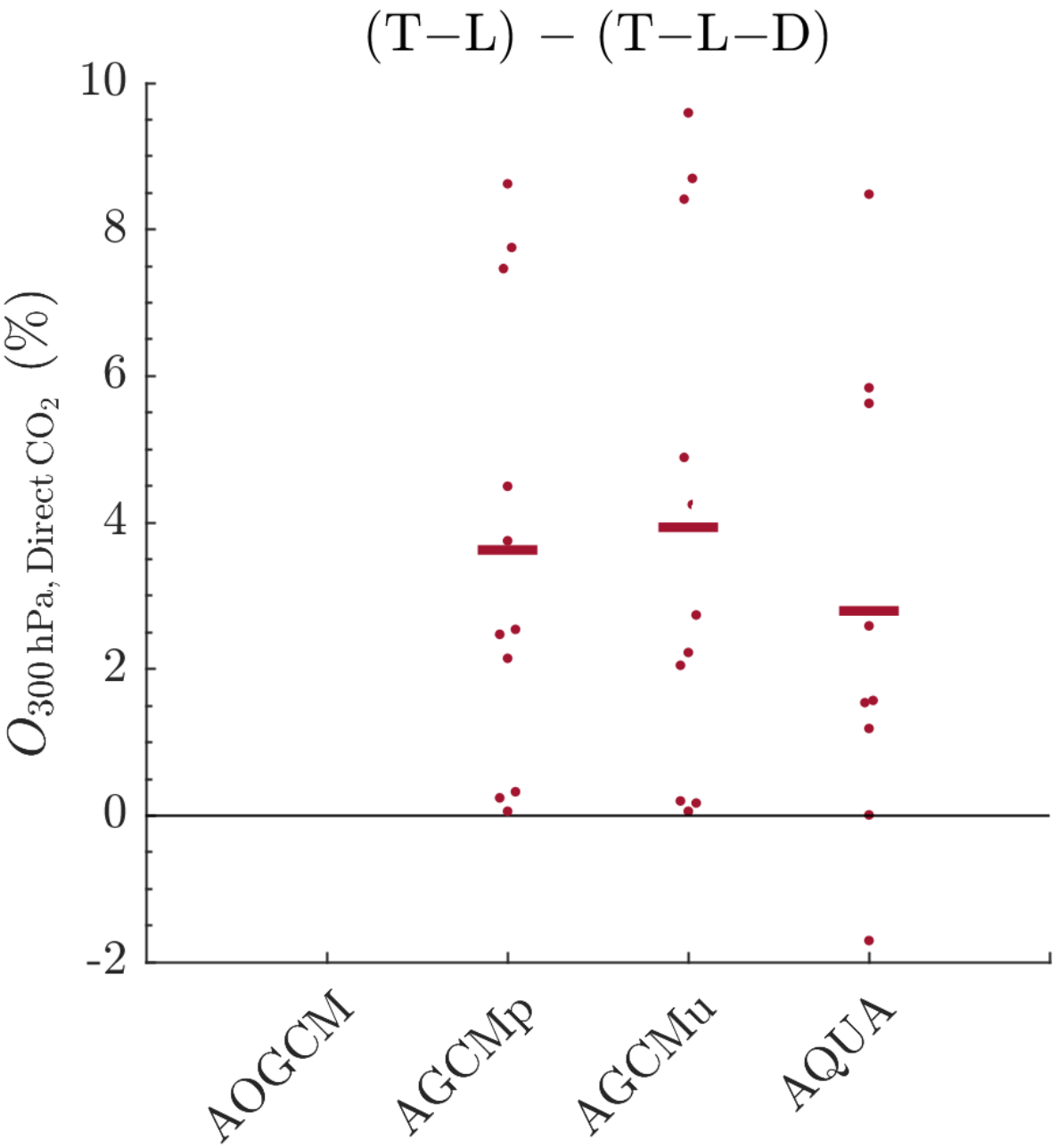

Figure S5. The difference in overprediction between the combined indirect plus the direct CO_2 response and only the indirect CO_2 response for each model across the model hierarchy (dots). The mean difference in overprediction is denoted by the horizontal line.

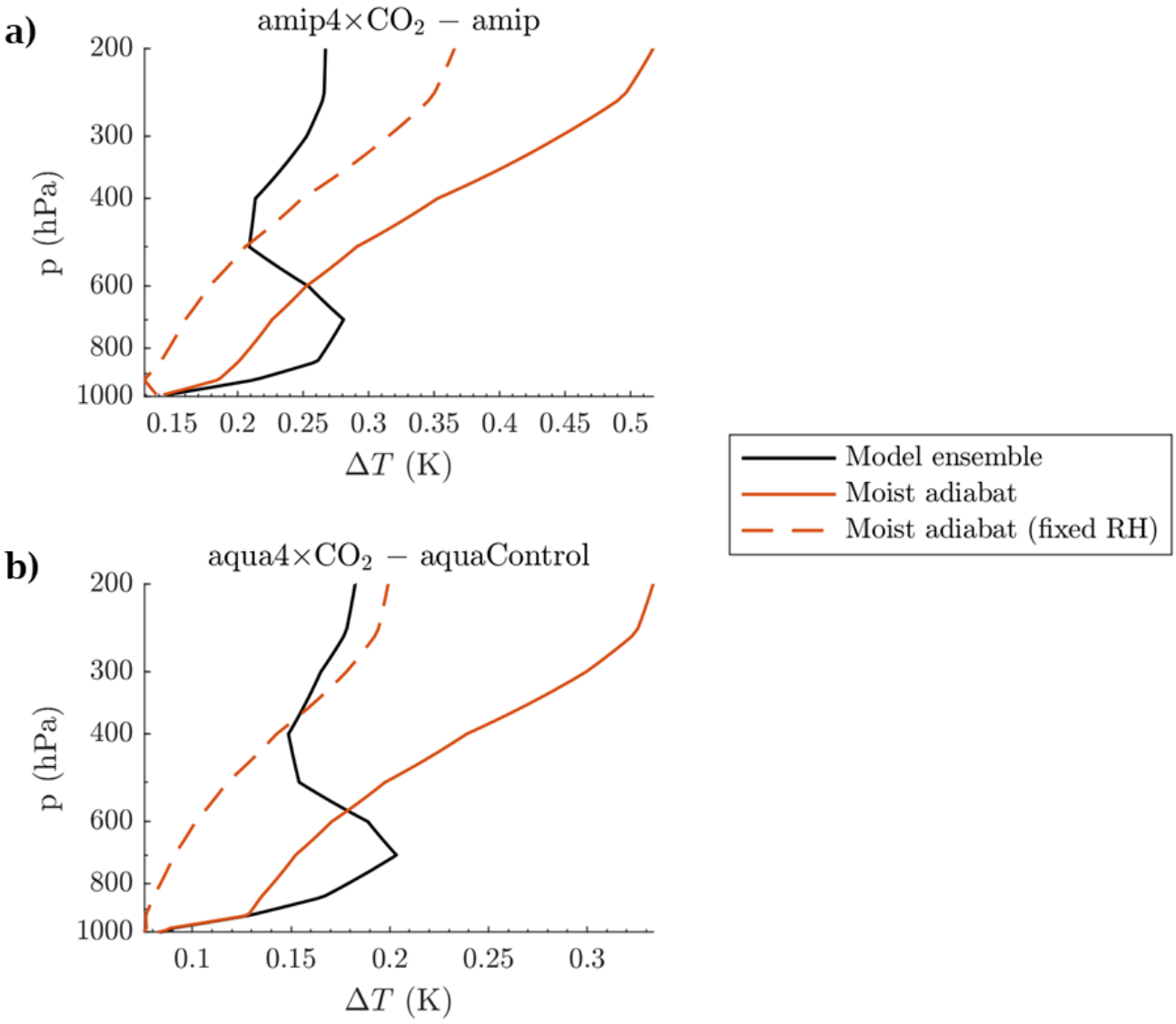

Figure S6. a) Vertical structure of the AGCM multi-model mean temperature response to the direct effect of CO_2 (black), the corresponding moist adiabatic prediction (solid orange), and the moist adiabatic prediction holding the 2 m relative humidity fixed at the climatological value (dashed orange). While the warming due to the direct effect of CO_2 is approximately uniform with height above the boundary layer in the multi-model mean, the moist adiabat predicts amplified warming aloft. b) is the same for AQUA.

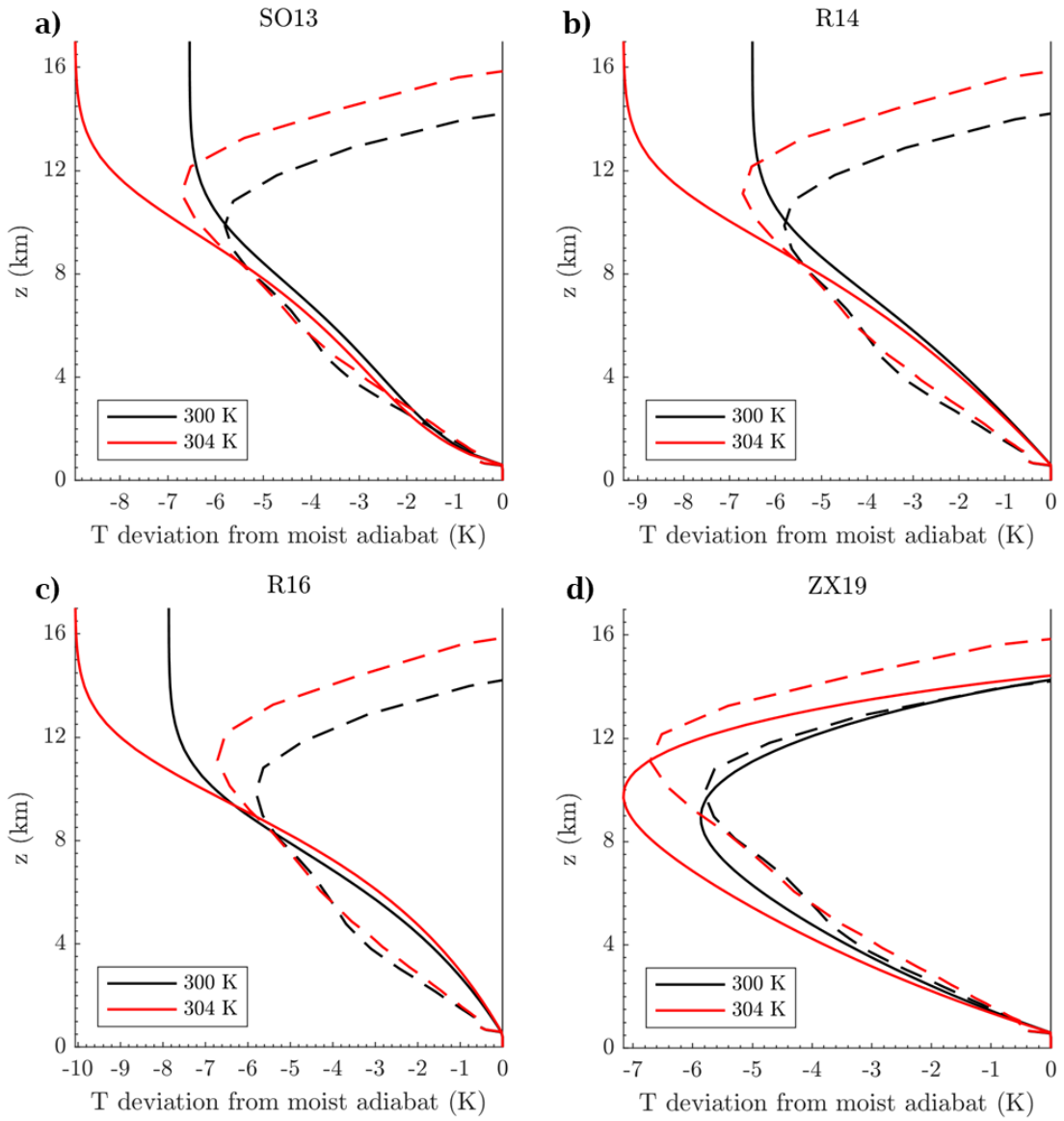

Figure S7. Temperature deviation from a moist adiabat in GFDLrce for a prescribed SST of 300 K (black dashed) and 304 K (red dashed). The corresponding predictions of the temperature deviations are shown for a) the SO13 zero-buoyancy bulk-plume model (solid) for $\hat{\epsilon} = 0.7$ and RH = 85%, b) the R14 zero-buoyancy bulk-plume model for $\epsilon = 0.3$ km^{-1} and $\alpha = 0.8$, c) the R16 zero-buoyancy bulk-plume model for $a = 0.25$ and PE = 1, and d) the ZX19 spectral-plume model for RH = 65%, $z_t = 14.61$ km, $\epsilon_0 = 0.33$ km^{-1}, and $k = 1.00$.

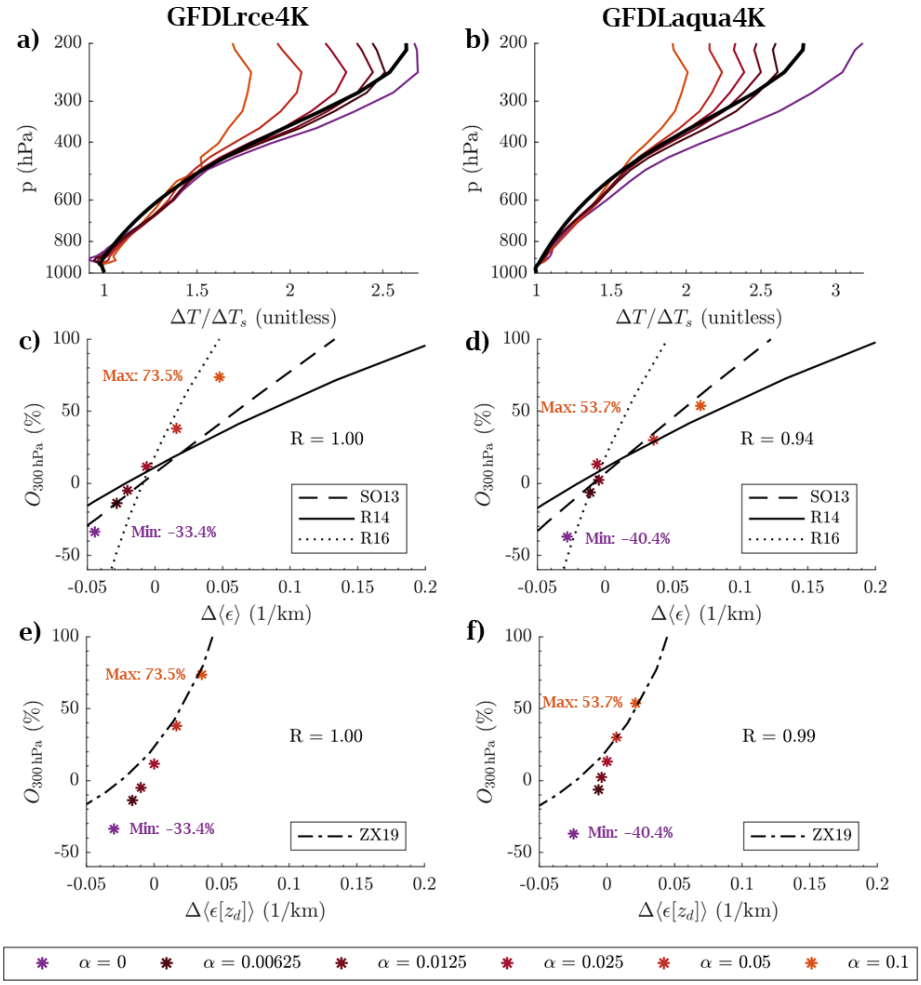

Figure S8. Temperature responses simulated in GFDL where the Tokioka parameter α is held fixed at 0.025 for the control climate and varied as shown only for the warm climate. The amplified warming in the upper troposphere strengthens when the entrainment weakens with warming in a) GFDLrce4K and b) GFDLaqua4K. The moist adiabatic response is shown as a thick black line for reference. Overprediction of the moist adiabat decreases with a weakening response of the vertically-averaged bulk-plume entrainment $\langle\epsilon\rangle$ with warming in both c) GFDLrce4K and d) GFDLaqua4K. e) and f) are similar except the x-axis is the vertically-averaged spectral entrainment rate $\langle\epsilon[z_d]\rangle$. The deviation as predicted by zero-buoyancy bulk-plume models of Singh and O'Gorman (2013) (labeled SO13), Romps (2014) (R14), Romps (2016) (R16), and the spectral plume model of W. Zhou and Xie (2019) (ZX19) are shown as black lines in panels c–f.